



## PÔVODNÁ PRÁCA – ORIGINAL PAPER

# The assessment of forest parameters by combined LiDAR and satellite data over Alpine regions – EUFODOS Implementation in Austria

## Hodnotenie parametrov lesa kombináciou LIDAR-u a satelitných údajov v alpských regiónoch – implementácia systému EUFODOS v Rakúsku

Mathias Schardt<sup>1,2</sup>, Klaus Granica<sup>1</sup>, Manuela Hirschmugl<sup>1</sup>, Janik Deutscher<sup>1</sup>, Michael Mollatz<sup>1</sup>, Martin Steinegger<sup>1</sup>, Heinz Gallaun<sup>1</sup>, Andreas Wimmer<sup>1</sup> and Stefanie Linser<sup>3\*</sup>

<sup>1</sup>Joanneum Research Forschungsgesellschaft mbH, Leonhardstraße 59, A–8010 Graz, Austria

<sup>2</sup>Graz University of Technology, Rechbauerstr. 12, A–8010 Graz, Austria

<sup>3</sup>European Forest Institute – Central-East European Regional Office c/o University of Natural Resources and Life Sciences, Feistmantelstr. 4, A–1180 Vienna, Austria

### Abstract

Regional authorities require detailed and georeferenced information on the status of forests to ensure a sustainable forest management. One of the objectives in the FP7 project EUFODOS was the development of an operational service based on airborne laser scanning and satellite data in order to derive forest parameters relevant for the management of protective forests in the Alps. The estimated parameters are forest type, stem number, height of upper layer, mean height and timber volume. RapidEye imagery was used to derive coniferous and broadleaf forest classes using a logistic regression-based method. After the generation of a normalised Digital Surface Model and a forest mask, the forest area was segmented into homogeneous polygons, tree tops were detected, and various forest parameters are calculated. The accuracy of such an assessment was comparable with some previous studies, and the R-square between the estimated and measured values was 0.69 for tree top detection, 0.82 for upper height and 0.84 for mean height. For the calculation of timber volume, the R<sup>2</sup> for modelling is 0.82, for validation with an independent set of field plots, the R<sup>2</sup> is 0.71. The results have been successfully integrated into the regional forestry GIS and are used in forest management.

**Key words:** LiDAR; satellite data; forest parameters; protective forests; Alpine environment

### Abstrakt

Regionálne plánovanie zabezpečujúce trvale udržateľný manažment lesa vyžaduje detailné a georeferencované informácie o stave lesov. Jedným z cieľov projektu EUFODOS (projekt 7. RP EÚ) bolo vyvinúť operatívnu službu využívajúcu údaje leteckého laserového skenovania v kombinácii so satelitnými údajmi, pomocou ktorých sú odvodené informácie potrebné pre obhospodarovanie ochranných lesov v Alpách. Zisťované parametre sú lesný typ, počet stromov, výška hornej korunovej vrstvy, priemerná výška a kmeňová zásoba. Použilo sa snímkovanie systémom RapidEye pre odvodenie tried ihličnanov a listnáčov s použitím logistického regresného modelu. Po vygenerovaní normalizovaného digitálneho modelu povrchu a masky lesa sa plocha lesa segmentovala do homogénnych polygónov, identifikovali sa vrcholce stromov a vypočítali sa požadované porastové charakteristiky. Presnosť uvedených odhadov bola porovnateľná s predošlými štúdiami – R<sup>2</sup> medzi odhadovanými a meranými hodnotami pozícií vrcholcov stromov bol 0,69, pre hornú výšku 0,82 a pre priemernú výšku porastu 0,84. Pri výpočte objemu dreva bol R<sup>2</sup> príslušného modelu 0,82. Pri validácii s nezávislým súborom plôch bola dosiahnutá hodnota R<sup>2</sup> 0,71. Prezentované výsledky sa úspešne integrovali do regionálnych lesníckych GIS sú využívajúce pri manažmente lesa.

**Kľúčové slová:** LiDAR; satelitné údaje; parametre lesa; ochranné lesy; prostredie Álp

## 1. Introduction

Forests play a key role in the European economy and environment. Their role includes diverse ecological and economic functions, which can be adversely affected by insect infestations, forest fires, storms or windfall events. Local or regional authorities thus require detailed and georeferenced information on forest degradation status to be able to take appropriate countermeasures against the aftermaths of forest damage and to ensure a sustainability of forest management. However, stand and site data are most often obtained by expensive ground-based surveys or time-consuming inventories (Schardt & Granica 2012). The terrestrial monitoring methods cannot ensure a full coverage since a complete inspection

of the whole area is not feasible using the available technical and personnel resources and within an acceptable time frame. Therefore, the FP7 EUFODOS services, based on remote sensing data, which were customized to users' needs, were developed to facilitate a precise localisation and effective assessment of forest damages as well as an operational derivation of desired forest parameters.

To secure that the service development is well responsive to user requirements all EUFODOS users were engaged in a User Executive Body (Linser 2011). The intensive cooperation between service providers and users facilitated the roll-out and uptake of the services by the users after the run-time of the project. The user, whose request are addressed in this study, is the Forestry Board of Styria, which requested a spe-

\*Corresponding author. Stefanie Linser, e-mail: [stefanie.linser@efi.int](mailto:stefanie.linser@efi.int)

cific service for deriving forest parameters from LiDAR and satellite data, which are needed for targeted management of Alpine protective<sup>1</sup> forests in order to maintain and enhance their protective function against natural hazards.

The objective of this study is to test the efficiency of EUFODOS services in the assessment of the following forest parameters: forest mask including the upper forest border line, forest types, stem number, height of upper layer, mean height and timber volume.

This study was initiated by the fact that most of the previously used forest inventory techniques aiming at these parameters relied on aerial photography and ground-based surveys, but could not be applied in larger regions due to limited resources. Further on, those surveys did not allow the derivation of spatial distribution of forest parameters. Our study strives to fill some methodological gaps in data collection and evaluation using advanced techniques of remote sensing.

## 2. Data and methods

### 2.1. Test region and data

The pilot test site is located in Upper Styria in the region of “Murtal”, with approximately 1600 km<sup>2</sup>, and is characterized by a high-mountainous terrain with elevation 800 – 2500 m a.s.l., which is prone to natural hazards. This region is mainly stocked with Austrian spruce (*Picea abies*), European larch (*Larix decidua*) and Scots pine (*Pinus sylvestris*), and in the higher parts of the subalpine tree line mixed with dwarf mountain pine (*Pinus mugo*) and green alder (*Alnus viridis*).

The LiDAR data were acquired between 2009 and 2012 using a Riegl LMS-Q560 sensor. The point cloud density amounts to 4 points/m<sup>2</sup> below 2000 m a.s.l. and 1 point/m<sup>2</sup> above this elevation limit. Aside from the LiDAR data, also CIR ortho-images were available for visual interpretation. The LiDAR data encompassed big data volumes in \*.las format (about 1.3 TB), making it necessary to transfer it via a hard disk.

RapidEye data was used for the classification of species composition (forest types). RapidEye covers five spectral bands, from 0.44µm – 0.73µm, with 6.5m spatial resolution and a very high revisit cycle based on the constellation of five satellites in the orbit. In order to cover the whole area, two data acquisitions were needed, one from July, 8<sup>th</sup>, 2010 and one from June, 16<sup>th</sup> 2012. Data costs for this imagery was 1€ per km<sup>2</sup> and distributed via an ftp link by the Blackbridge company.

Additionally, field measurement campaigns aiming at the collection of reference data for the LiDAR based assessment of forest biomass, respectively timber volume, were performed applying “Bitterlich Sampling” (Schreuder 1993). Altogether 99 field plots were collected by the field team. For this field campaign the base equipment comprised a relascope, an altimeter (Vertex), and a calliper. The forest experts made measurements to obtain the following parameters:

- Number of trees
- Tree species
- Diameter at breast height
- Mean height (the mean tree of all measured diameters)
- Upper Height (the mean tree of the three strongest trees)
- Crown projection

Based on these field measurements a number of forest parameters were calculated, as there are the basal area of the trees, the number of the trees and the timber volume.

### 2.2. Derivation of forest parameters from LiDAR and satellite data

An approach combining LiDAR and satellite data was followed to achieve the aims in a cost-effective way. Three-dimensional structural parameters, such as height, stem numbers and timber volume were derived from LiDAR data, whereas information on the distribution of forest types (species) have been assessed by means of optical satellite remote sensing imagery.

### 2.3. Satellite data classification

Two RapidEye satellite scenes were used for the differentiation of coniferous and broadleaf classes. The used classification method consisted of the following steps:

- individual image bands were fine registered as only bands 1, 2 and 3 were geometrically coherent while bands 4 and 5 differed. Thus, a dense image matching was performed between band 1 to band 3 to obtain the shift vectors.
- ground control points (GCPs) were manually measured in the resulting RapidEye image using a reference orthophoto and a digital terrain model. The GCPs were then utilized to adjust the initial sensor model followed by the adjusted sensor model to WGS84 UTM33 North projection.

Reference data sets were derived by visual interpretation of CIR orthoimagery and digitized into a vector file (shp). The classification was based on logistic regression (see Jost 2006). The logistic regression is a type of probabilistic statistical classification model, which predicts the probability of a binary response. The formula of the logistic regression model is:

$$P(x) = \frac{e^{\eta}}{1 + e^{\eta}} \quad \text{with} \quad \eta = \beta_0 + \beta_1 x_1 + \dots + \beta_n x_n$$

$P$  – probability of occurrence of an event (percentage of deciduous trees)

$e$  – exponential function

$\eta$  – linear predictor

$\beta$  – regression coefficients

$x$  – predictor variables (spectral values)

For the calculation of the regression coefficients the response vector and the predictor variables are required. The percentage of deciduous trees of the reference data serve

<sup>1</sup> The management supports soil protection, water quality and quantity and other forest ecosystem functions, or protects the infrastructure and natural resources from natural hazards.

as response vector and the spectral values of the reference data serve as predictor variables. In the next step the spectral values of the high resolution image and the logistic regression coefficients are used to classify the image data. The regression delivers for each pixel a percentage of deciduous trees from which the final forest type map is derived.

In a post-processing step the classification result was aggregated on pixel basis into three classes (see Table 1).

**Table 1.** Threshold Values for the three Forest Types Classes.

| Class        | Percentage of broadleaved trees |
|--------------|---------------------------------|
| Coniferous   | 0 to <25                        |
| Mixed forest | 25 to 75                        |
| Broad-leaved | > 75 to 100                     |

2.4. LiDAR Data Processing

A workflow starting from the raw LiDAR point cloud and ending with the resulting forest parameter map is presented in Fig. 1. The most important processing steps are the delineation of the forest border, the detection of tree tops, the segmentation of homogeneous forest stands and finally the calculation of all forest parameters. The entire workflow is operated as an automated procedure implemented in the Joanneum Research in-house software package IMPACT as the “IMPACT LiDAR Toolbox”.

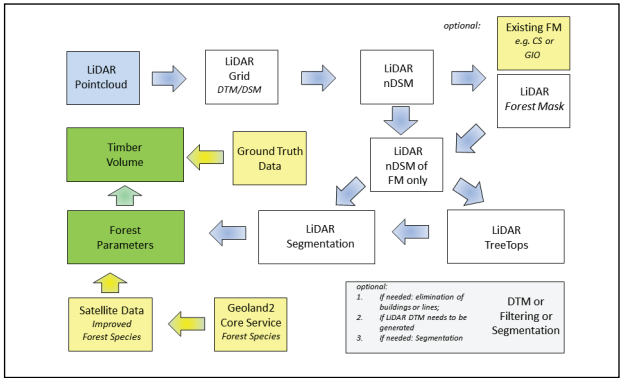


Fig. 1. Workflow for LiDAR data processing.

The digital terrain model (DTM) and the digital surface model (DSM) were imported into a raster file from the original point cloud data (available in \*.las format) with spatial resolution of 50 cm. Then, a normalized digital surface model (nDSM) was derived as the difference between the digital surface model and the digital elevation model. A forest mask is derived from the nDSM. The nDSM within the forest mask is then used for tree top detection, segmentation, forest parameters and tree volume calculations. The following parameters were derived for each polygon (generated by the segmentation procedure) in the region:

- Trees per hectare
- Coniferous/broadleaf percentage
- Upper and mean tree heights
- Exposition, slope, height above sea level
- Canopy space integral

This canopy space integral is defined as the sum of all vegetation heights in a forest segment and it serves as an

intermediate parameter, which is later on used as input variable to derive the timber volume.

2.4.1 Generation of Forest Border and Forest Mask

The forest border line was derived according to the forest definitions by the Styrian Forest Administration: i.e. minimum crown cover of trees is 10 %, minimum tree height above 1.3 m, minimum distance between stocked areas is 10 m, minimum stocked (> 10% crown closure) area of 1000 m², and minimum un-stocked area of 1000 m². Further, a separation of shrub-land (dwarf mountain pine, green alder stands and succession areas) was performed by applying the same generalization procedure in addition with a “maximum potential tree height” below 5 m.

Settlements and water areas are automatically excluded using morphological operations based on the classified LiDAR point cloud. Then crown cover is calculated over segments with a minimum size of 1000 m² (specified by the Styrian user). The crown cover is thereby defined as the proportion of the forest floor covered by the vertical projection of the tree crowns over the respective segments. Within areas with a crown cover above the specified “minimum crown cover” parameter, aggregation according to the specified “minimum distance between stocked areas” is applied.

Next a generalization is performed according to the “minimum stocked area” and “minimum unstocked area” parameters by applying standard morphological operations. As a result, stocked areas are delineated. Only the LiDAR data is used as input to these automatic processing steps.

Often, the forest area definition requires taking into account further nomenclature constraints, such as incorporation of temporarily un-stocked areas into forest land or exclusion of tree covered areas according dominant land-use (e.g. parks, orchards, arable land with trees). To incorporate such additional constraints into the generalization process, visual refinement of the automatically derived results was performed.

2.4.2 Tree Top Detection

The Tree Top Detector automatically detects tree tops based on the LiDAR nDSM as input. The method uses a multi-scale Laplacian of Gauss (LoG) method, which is a combination of the Laplacian and Gauss filter (Gonzalez & Woods 2002). The procedure consists of the following five steps (the intermediate results are shown in Fig. 2). First, the LoG is used to blur the image, with the degree of blurring being determined by the value of the standard deviation ( $\sigma$ ). The procedure used here involves three scales of LoG filtering based on three different  $\sigma$  values (2, 3, 4) in order to detect trees of different size. The results of the LoG filtering with different  $\sigma$  are depicted in Fig. 2b), (c) and (d). An appropriate sigma value was selected on the basis of Chen et al. (2006). Second, the original nDSM is processed using a simple LMA (Local Maxima Approach) (Fig. 2e). Third, the LoG images are weighted according to their respective level ( $\sigma$ ) and then added (Fig. 2f). Fourth, intensity maxima are



detected using LMA in the image produced in the previous step (Fig. 2g). Fifth, the intensity maxima are dragged to their nearest height maximum (result from the step 2) (Fig. 2h) (Hirschmugl 2008).

### 2.4.3 Derivation of Homogeneous Forest Segments

Within the test site a segmentation procedure is applied to divide the forest into relatively homogeneous forest segments based on the input nDSM and an existing set of forest roads. The resulting forest segments represent a homogeneous dominant height and vertical forest structure. In order to ensure similar tree height the nDSM is used. For assessing

the vertical stand structure, a minimum variance wedge filter is calculated. These two data sets are then stacked to one image and used in a three-step region growing image segmentation procedure to derive polygons of homogeneous forest segments. The first step is a coarse segmentation, which derives the main skeleton of segments. This coarse segmentation uses the input files down-sampled to 5 m spatial resolution and smoothed by symmetric nearest neighbor (SNN) filter. The result shows the main borders, but the polygons do not exactly correspond to the tree crown outlines. Therefore, in a second step, a fine-segmentation is performed using the full resolution data and resulting in a clear over-segmentation of the forest, but representing a more exact delineation along the tree crowns.

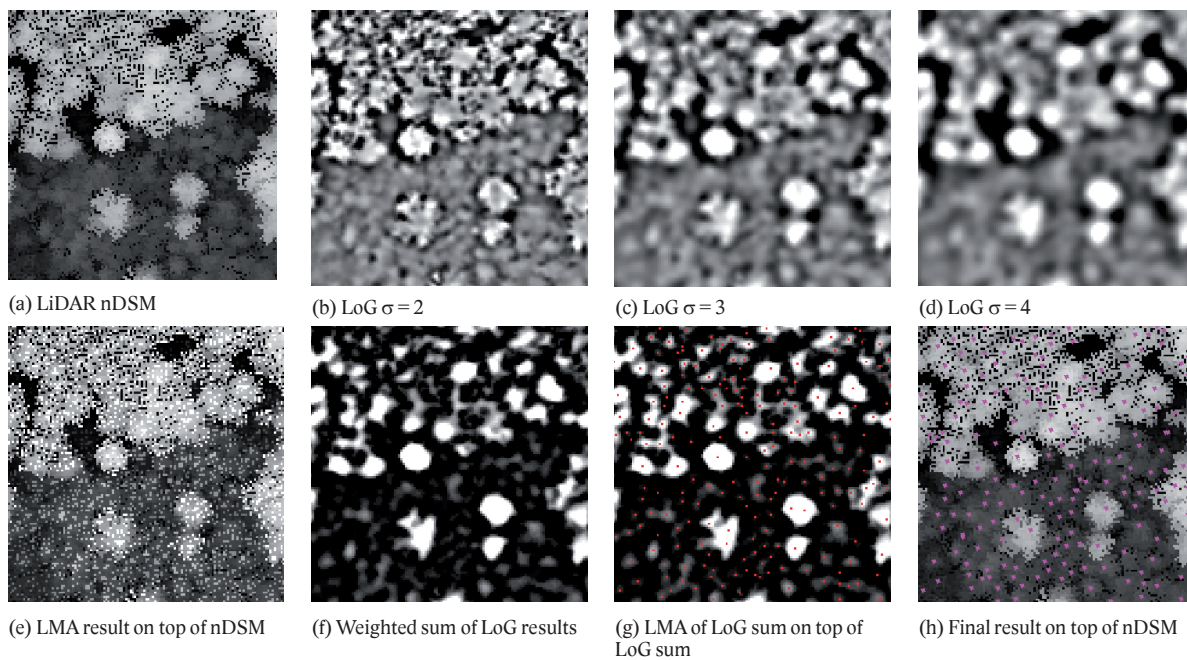


**Fig. 2.** Processing steps and intermediate results for the LoG approach based on LiDAR nDSM data. Source: Hirschmugl (2008).

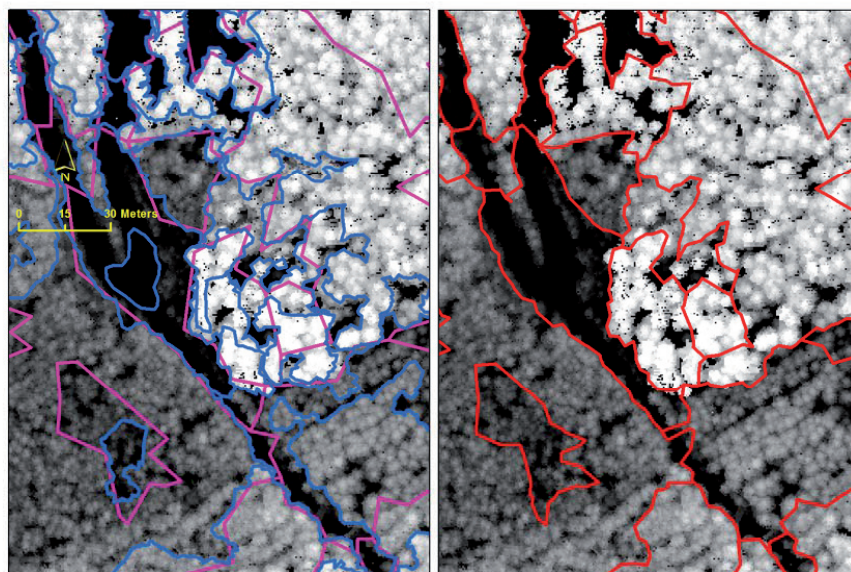


**Fig. 3.** Refinement of segmentation outlines: left: pink – coarse segmentation, blue – fine segmentation, right: red – combined result.

In the third step, the two results are combined by snapping the coarse segment borders to the fine segmentation outlines (Fig. 3). The pink lines are the coarse segment borders and the blue lines are the fine segment borders. After the combination, the resulting borders (red) are automatically adapted as long as the distance to the original line is below a user defined threshold, which was set to one meter in the current case.

The final forest segments (Fig. 4) are used to calculate the forest parameters within each polygon.

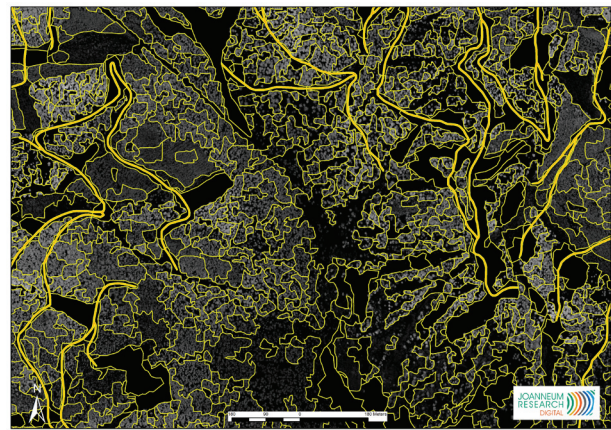


**Fig. 4.** A subset of the segmentation result showing forest stand borders (yellow lines).

2.4.4 Derivation of Forest Parameters

First, based on the tree top detections, the stem numbers per segment and per ha are calculated. Second, based on both the tree top detections and their respective tree heights within each segment, three different forest segment height values are calculated: Height of upper layer (i.e. the mean height of 20% highest trees per segment), mean height (i.e. the mean height of all detected trees) and height of second layer, if existing (i.e. the mean height of the 20% highest trees of the second layer, which are trees smaller than 2/3 of the height of the upper layer). Third, mean slope, main aspect and mean height above sea level are calculated for each segment.

Finally, timber volume is calculated for each segment using parameter settings proposed by Hirschmugl et al. (2013). They tested different variables i.e. those specifying the link between the ground-based reference data and the LiDAR-based variables for their suitability to estimate timber volume. Individual variables and combinations of variables available from the forest parameters processing were tested, e.g. height of upper layer, mean height, canopy cover, height above sea level, and the so-called ‘canopy space integral’, which is defined as the sum of all vegetation heights in a forest segment. The canopy space integral derived from LiDAR data gave the best results (Hirschmugl et al. 2013) and were thus used in the current study. From the 99 field plots, a listed sampling was done, where the plots were listed according to the timber volume. Every third plot was assigned as validation data and thus omitted from the modelling. The remaining plots served as reference data to build the regression model (Fig. 5). The regression using these 66

reference data sets yield the  $R^2$  of 0.82. The given equation was used to compute the timber volume for the entire area.

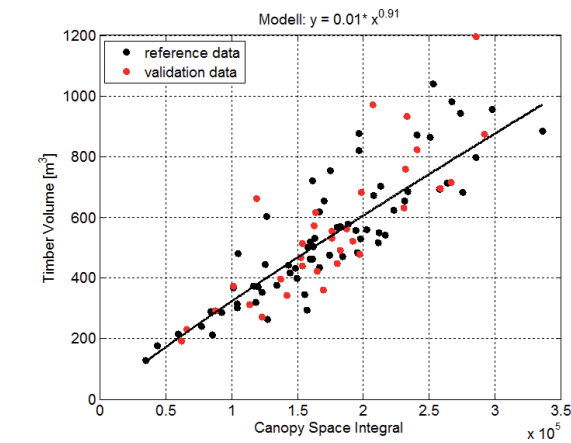


**Fig. 5.** Regression between timber volume and canopy space integral.

3. Results

3.1. Classification of Forest Types

The fine-registration of bands 1, 2 and 3 with bands 4 and 5 was performed before the geocoding. As topographical distortions were detected in a flight direction (Table 2), the bands 4 and 5 were registered employing the determined shifts.

**Table 2.** Statistics of automatically determined shifts in pixels between the image bands (in pixels).

|      | Along track | Across track |
|------|-------------|--------------|
| Mean | −0.03       | −0.00        |
| Std  | 0.63        | 0.07         |
| Min  | −3.37       | −1.57        |
| Max  | 2.75        | 1.78         |

After the fine-registration, the 50 ground control points (GCPs) were manually measured in the resulting RapidEye image using a reference ortho-photo and a digital terrain model. The GCPs were then utilized to adjust the initial sensor model yielding the accuracy given in Table 3. The geocoding was then performed with the adjusted sensor model to 5 meters GSD (Ground Sampling Distance) in WGS84 UTM33 North projection.

**Table 3.** Accuracy of the 50 GCPs after sensor model adjustment given in meters.

|      | Res-X  | Res-Y  | Length |
|------|--------|--------|--------|
| RMS  | 4.40   | 3.85   | 5.85   |
| Mean | 0.00   | 0.00   | 5.00   |
| Std  | 4.40   | 3.85   | 3.05   |
| Min  | −11.05 | −11.50 | 0.45   |
| Max  | 10.45  | 9.60   | 13.20  |

The quality of the resulting pixel-based forest-type map was assessed by an independent verification. The 57 verification areas were selected and interpreted in the same way



as the training areas (see above). For each verification area, the mean percentage of broad-leaved trees was calculated. All pixels of this area then were assigned to the corresponding forest type. Finally, all reference pixels (i.e. all pixels which are included within a verification area) were compared by means of a contingency matrix.

**Table 4.** Accuracy of forest type classification: pixel count.

| Pixel count  | Classified |              |             |       |
|--------------|------------|--------------|-------------|-------|
| Reference    | Coniferous | Mixed Forest | Broadleaved | Sum   |
| Coniferous   | 17648      | 1192         | 0           | 18840 |
| Mixed forest | 1387       | 6126         | 1133        | 8646  |
| Broadleaved  | 0          | 293          | 1150        | 1443  |
| Sum          | 19035      | 7611         | 2283        | 28929 |

**Table 5.** Accuracy of forest type classification: percent.

| Percent      | Classified |              |             |
|--------------|------------|--------------|-------------|
| Reference    | Coniferous | Mixed Forest | Broadleaved |
| Coniferous   | 92.71      | 15.66        | 0.00        |
| Mixed forest | 7.29       | 80.49        | 49.63       |
| Broadleaved  | 0.00       | 3.85         | 50.37       |

The overall accuracy counts for 86.16%. Whereas coniferous forest could be classified very well, major deviations occurred between mixed forest and broadleaved forest. In general, the area of broadleaved forest was overestimated (ref. Table 4).

3.2. Forest Border and Forest Mask

After the derivation of the Alpine tree line, the forest mask was derived using an automated approach. The processing result was then revised by visual control due to ambiguous borders and areas which could not be derived using the automated processing. A quality control has been performed by random sampling with 298 sampling points. The forest and non-forest areas were compared by visual interpretation of LiDAR and CIR aerial imagery according to defined nomenclature specifications. The result shows an overall accuracy of almost 99% (Table 6).

**Table 6.** Accuracy assessment of the forest mask.

|                       | 0 – No forest | 1 – Forest | User accuracy [%] |
|-----------------------|---------------|------------|-------------------|
| 0 – No forest         | 90            | 0          | 100.00            |
| 1 – Forest            | 3             | 205        | 98.56             |
| Producer accuracy [%] | 96.77         | 100.00     |                   |
| Overall accuracy [%]  |               |            | 98.99             |

3.3. Forest Stand Segmentation

The forest area was divided into homogeneous forest patched by automatic segmentation. The result is shown in Fig. 6 a). A quantitative evaluation of such an automated segmentation result is a rather impossible task, as there is no absolute ground truth. Therefore, the result is visually compared to an independent visual-manual segmentation done by an experienced interpreter (Fig. 6 b). There are two main differences: first, the automated segmentation produces smaller segments, especially in the areas of low canopy cover or close

to the upper forest border. Second, the automatic segmentation outline is – due to the refinement step – much more detailed than the manual segmentation result. The differences between the two results are shown in Fig. 6.

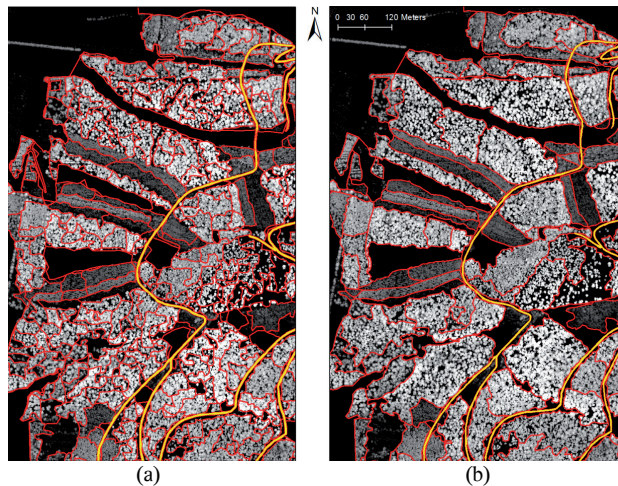


**Fig. 6.** Comparison of lines derived using the automated segmentation (a) and using the visual interpretation (b). Forest roads are displayed in yellow color.

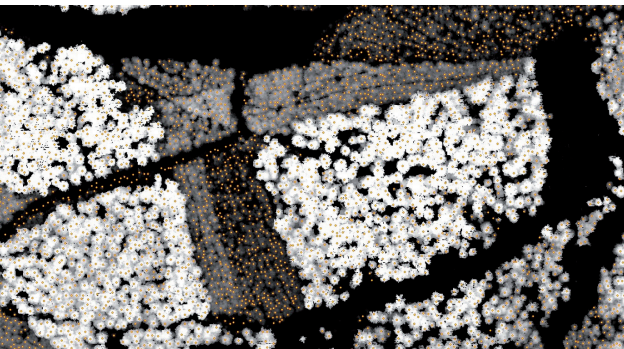


**Fig. 7.** Result from the tree top detection.

3.4. Tree Top Detection

Figure 7 shows the result of the tree top detection in an area of forest stands with different growth classes. For accuracy assessment, the result is compared with stem numbers estimated in the field. An evaluation could not be done on an individual tree basis, because the field survey did not provide the data on all trees. Instead, a stand wise comparison, based on the field plots, was applied. Comparing the stem numbers of all plots with the number of trees detected automatically led to  $R^2$  of 0.54 (Fig. 8 a). The figure suggests that the automatic approach is not able to detect all trees in very dense forests (above 1500 stems/ha). Therefore, plots above 1500 stems/ha were omitted, which increase the  $R^2$  to 0.69 (see Fig. 8 b). In terms of mean difference, the error decreased from 33% for all plots to 30% when the dense plots were removed.

3.5. Forest Stand Parameters

For each of the segments, the height of the upper layer and the mean height were calculated. Fig. 9 shows the comparison of the mean heights derived from the LiDAR data compared to the field measured mean height. The  $R^2$  is 0.84. The

$R^2$  for upper height is 0.82. Fig. 10 shows the map result exemplarily for the upper height per polygon.

Finally, timber volume was calculated per stand based on the canopy space integral and the field plot data. From the altogether 99 field plots of the ground truth campaign, one third of the plots were used for the validation. The analysis showed an  $R^2$  of 0.71.

A further comparison of the calculated timber volume for managed forests over the entire “Murtal” region with the official numbers from the public Authorities showed that the numbers correlate quite well, i.e. 29277 solid cubic meters vs. 30333 solid cubic meters, respectively (BFW 2009).

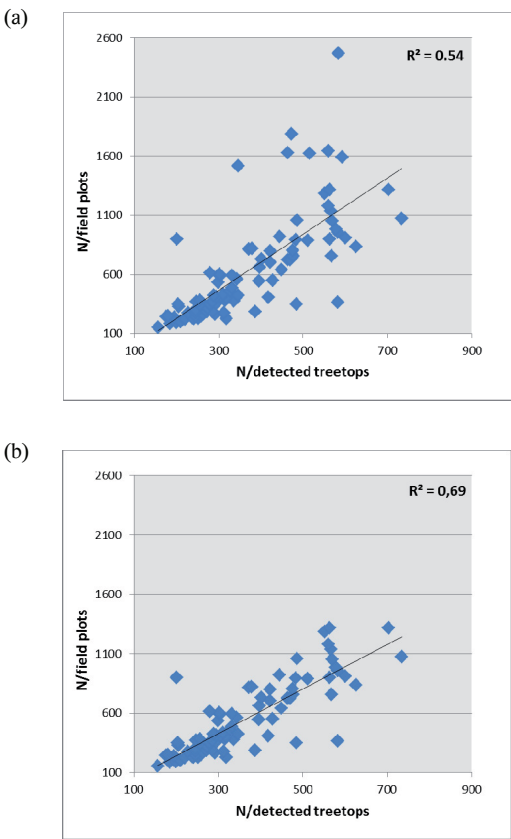


**Fig. 8.** Comparison of stem numbers per ha using a) all field plots and b) only field plots with less than 1500 trees/ha.

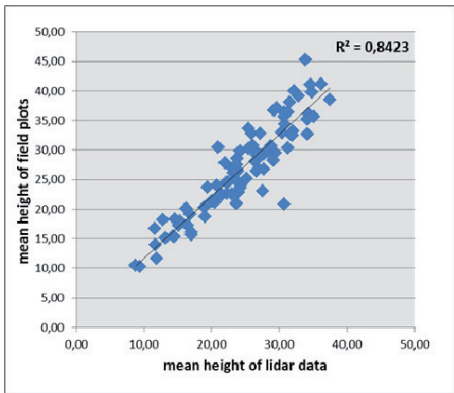


**Fig. 9.** Comparison of mean height from field plots and derived from LiDAR data.

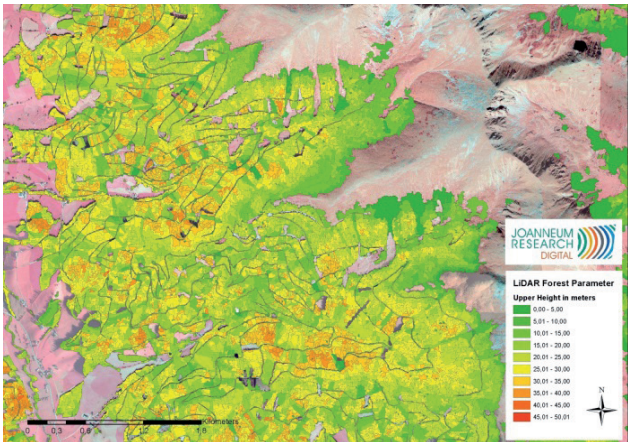


**Fig. 10.** Subset showing the upper height in meters per stand.

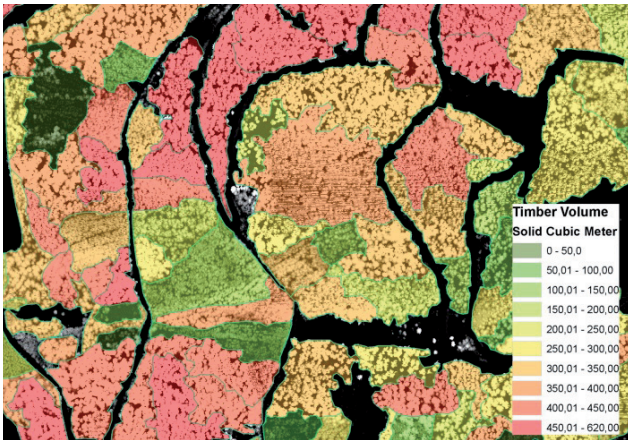


**Fig. 11.** Subset for the derivation of timber volume (in solid cubic meters).

#### 4. Discussion

New and innovative LiDAR tools have successfully been adapted and implemented due to the user’s feedback within the development of the service. An important module, urgently requested by the forest experts, is that on segmentation, which was used to derive the homogeneous forest segments. The segmentation was automatized to meet the requirements of forest experts. A comparison with the conventionally derived stand borders showed two main differences: first, the automatic segmentation led to smaller and thus more segments than an interpreter would be able to delineate. Considering the use of the segments, this over-segmentation does not pose a problem, because in further analysis, neighbouring patches with similar forest attributes can be merged, if more generalized maps are needed. Second, the outlines of the automated segmentation are much more detailed than the conventional segmentation. This detailed outline is actually an advantage for the following automatic processing, because straight lines as usually done by manual segmentation tend to cut trees in half leading to errors in the calculation of the forest parameters, especially for height of dominant layer and timber volume. The current segmentation procedure utilizes the nDSM and the forest roads, but in future, additional inputs, such as optical data can be used to ensure the segments are homogeneous in terms of tree height



and structure as well as in terms of species composition or forest types (coniferous/broadleaf).

The derivation of forest border at the upper forest borderline can be considered as a challenging task. Several rules have been tested to obtain a proper forest border, e.g. different distances between single trees or crown coverage thresholds. At the same time, the results were evaluated in field excursions and validated by the user. The validation showed that the forest border is highly accurate with almost 99% overall accuracy and therefore this approach can be considered as superior to previous forest masks, which were generated from satellite or orthophoto data, where an overall accuracy reached 96% (Gallaun et al. 2007).

The overall accuracy for the classification of forest types is 86.16%. Iost (2006) used this method for forest-non-forest classification and for the determination of the mixture of coniferous and broadleaved trees. He achieved an accuracy of 94.1% for the forest non-forest map and 75% – 83% for the forest type classification.

The tree top detection was performed in a fully automatic manner with expected accuracy. Analysis showed that trees in very dense stands are most prone to omission error. Our mean difference results of 33% (all plots) respectively 30% (plots with < 1500 stems/ha) are worse than previously achieved accuracies reported by Sačkov et al. (2014), who showed an mean difference of 11%. One reason for this difference might be the density of the forest: in Sačkov et al. (2014) the stand with the highest density had a stem number of 1000 stems/ha, while in our test area, there are 23 plots with stem numbers above 1000 stems/ha. Another reason might be the type of field data used for comparison: while Sačkov et al. (2014) could rely on full assessment of all individual trees, our stem numbers are only modelled based on the measured Bitterlich samples. Finally, Sačkov et al. (2014) used the full LiDAR point cloud data, while our approach is based on the nDSM. Quality control was also done visually by both the developers and the users. The evaluation showed that tree tops from almost all visible trees could be detected but small trees hidden beyond larger tree crowns are typically omitted. This has already been found by other authors (Sačkov et al. 2014; Kaartinen & Hyppä 2008). The most important advantage of the developed Tree Top Detector is its independence from tree models, i.e. no a-priori information about tree species is necessary. Finally, based on the current results further investigations are foreseen to evaluate the detection rate also in relation to species composition and age classes.

Another important product was the computation of maps showing the timber volume for each polygon. For reference a set of “Bitterlich” samples has been acquired, that is on the one hand needed to establish the regression model and on the other hand used to verify the results. In order to properly correlate the sampling results and the LiDAR data results, several issues have to be kept in mind: (i) different growth environments need representative and comprehensive sampling, (ii) changes between LiDAR data acquisition and field work have to be detected and (iii) to select representative samplings in the preparation of the field maps to avoid inconsistency in the field data, which could happen if field campaigns are performed by different people. With

this respect, the EUFODOS experience confirmed previous applications (Clementel et al. 2011), but also showed optimization potential especially with regard to the missing information of age classes. However, the accuracies of the timber calculations were in line with the calculations from existing investigations (Hollaus 2009; Wack 2006) and correlate quite well with official numbers.

Stand height maps, with upper height and mean height, were also produced with accuracies ( $R^2$ ) of 0.82 and 0.84 respectively, because these are important parameters for the forest GIS. The above presented method and results showed that LiDAR data are an excellent source for the derivation of this parameter type, which is confirmed from previous studies (Means et al. 2000; Wack 2006).

## 5. Conclusions

The Styrian Forestry Board is not in the position to realize in situ surveys on forest parameters over large areas because field assessments are time and resource consuming. Therefore, the experts from Styrian Forestry Board decided to use remote sensing based methods for the derivation of the required forest parameters.

The results in the Austrian test case within the EUFODOS project proved that it is possible to derive forest parameters over large regions using a combined approach of LiDAR and satellite data. The regional Forestry Board of Styria approved these results and confirmed that they have received valuable data for improving their management tasks within protective forest areas. In EUFODOS a processing line for the derivation of forest parameters from high-resolution LiDAR data was developed and implemented into an operational toolbox. The EUFODOS LiDAR toolbox is now in an operational status and is disposed for commercial selling (Schardt 2014).

## Acknowledgements

*The EUFODOS project was co-funded by the European Union's Seventh Framework Programme for Research & Innovation Space, “Stimulating the Development of Downstream Global Monitoring for Environment and Security Services” (SPA.2010.1.1-01. (European Communities 2011)).*

## References

- BFW, Bundesforschungs- und Ausbildungszentrum für Wald, Naturgefahren und Landschaft, 2009: Die österreichische Forstinventur 2007–2009, Seckendorff-Gudent-Weg 8, Wien, Available at: <<http://bfw.ac.at/rz/wi.auswahl>>.
- Chen, Q., Baldocchi, D., Gong, P., Kelly, M., 2006: Isolating individual trees in a savanna woodland using small footprint lidar data – Photogrammetric Engineering and Remote Sensing 72: 923–932.
- Clementel, F., Colle, G., Farrugia, C., Floris, A., Scrinzi, G., Torresan, Ch., 2011: Estimating forest timber volume by means of “low-cost” LiDAR data - Italian Journal of Rem. Sens., 44:125–140. Available at: <[http://www.academia.edu/2018708/Estimating\\_forest\\_timber\\_volume\\_by\\_means\\_of\\_low\\_cost\\_LiDAR\\_data](http://www.academia.edu/2018708/Estimating_forest_timber_volume_by_means_of_low_cost_LiDAR_data)>.



- European Communities, 2011: EUFODOS European Forest Downstream Services – Improved Information on Forest Structure and Damages. GMES Downstream Services. Available at: <[http://ec.europa.eu/enterprise/policies/space/files/eufodos\\_en.pdf](http://ec.europa.eu/enterprise/policies/space/files/eufodos_en.pdf)>.
- Gallaun, H., Schardt, M., Linser, S., 2007: Remote Sensing based Forest Map of Austria and derived Environmental Indicators. In: Proceedings of the International Conference on Spatial Application Tools in Forestry (ForestSAT 2007). Montpellier, France.
- Gonzalez, R.C., Woods, R. E., 2002: Digital Image Processing. Prentice Hall, Inc., Upper Saddle River, New Jersey, second edition, 793 p.
- Hirschmugl, M., 2008: Derivation of Forest Parameters from UltracamD Data. Dissertation. Technische Universität Graz, Austria, 200 p.
- Hirschmugl, M., Gallaun, H., Wack, R., Granica, K., Schardt, M., 2013: EUFODOS: European Forest Downstream Services – Improved Information on Forest Structure and Damage – Int. Arch. Photogramm. Remote Sens. Spatial Inf. Sci., XL-1/W1: 127–131.
- Hollaus, M., Dorigo, W., Wagner, W., Schadauer, K., Hoefle, B., Maier, B., 2009: Operational wide-area stem volume estimation based on airborne laser scanning and national forest inventory data - Int. Journal of Rem. Sens., 30/19:5159–5175.
- Iost, A., 2006. Untersuchung der Eignung logistischer Regressionsmodelle zur Kartierung forstlicher Merkmale mit Satelliten-Fernerkundungsdaten. Hamburg, Germany.
- Linser, S., 2011: User Engagement in EUFODOS. EUFODOS Newsletter 1/2011. Available at: <[http://www.eufodos.info/sites/default/files/downloads/EF-First%20newsletter\\_02%2003%202011.pdf](http://www.eufodos.info/sites/default/files/downloads/EF-First%20newsletter_02%2003%202011.pdf)>.
- Means, J. E., Acker, S. A., Brandon, J. F., Renslow, M., Emerson, L., Hendrix, Ch. J., 2000: Predicting Forest Stand Characteristics with Airborne Scanning LiDAR - Photogr. Eng. & Rem. Sens, 66:1367–1371.
- Sačkov, I., Bucha, T., Kiraly, G., Brolly, G., Raši, R., 2014: Individual tree and crown identification in the danube floodplain forests based on airborne laser scanning data, EARSeL 34<sup>th</sup> Symposium Proceedings, Warsaw, 16–20 June 2014, p. 6.20–6.26.
- Schardt, M., Granica, K., 2012: Success Stories – Improved Information on Forest Structure and Damages. In: Discover what GMES can do for European regions and cities. Window on GMES. A GMES4Regions Publication. Special Issue November 2012.
- Schardt, M., 2014: European Forest Downstream Services – Improved Information on Forest Structure and Damages. Final Report to the European Commission Research and Innovation DG.
- Schreuder, H., Wood, G., Gregoire, T., 1993: Sampling Methods for Multiresource Forest Inventory, John Wiley & Sons, p. 117.
- Wack, R., 2006: Assessment of Alpine Protection Forest Parameters based on LiDAR Data and SPOT V Satellite Imagery. Proceedings of the HMRSC Workshop Graz, Austria.